JOURNAL OF AGRICULTURAL AND FOOD CHEMISTRY

More Toxic and Photoresistant Products from Photodegradation of Fenoxaprop-*p*-ethyl

JING LIN, JINGWEN CHEN,* YING WANG, XIYUN CAI, XIAOXUAN WEI, AND XIANLIANG QIAO

Key Laboratory of Industrial Ecology and Environmental Engineering (MOE), Department of Environmental Science and Technology, Dalian University of Technology, Linggong Road 2, Dalian 116024, P. R. China

The photodegradation pathway of the commonly used herbicide fenoxaprop-*p*-ethyl (FE) was elucidated, and the effects of the photodegradation on its toxicity evolution were investigated. Under solar irradiation, FE could undergo photodegradation, and acetone enhanced the photolysis rates significantly. The same photoproducts formed under the irradiation of $\lambda > 200$ nm and $\lambda > 290$ nm through rearrangement, loss of ethanol after rearrangement, de-esterification, dechlorination, photohydrolysis, and the breakdown of the ether linkages. One of the main transformation products, 4-[(6-chloro-2-benzoxazolyl)oxy] phenol (CBOP), was resistant to photodegradation under the irradiation of $\lambda > 290$ nm, and its photolysis rate was seven times slower than the parent under the irradiation of $\lambda > 200$ nm. Among the metabolites, CBOP (48 h EC_{50} of 1.49−1.64 mg/L) and hydroquinone (48 h EC_{50} of 0.25−0.28 mg/L) were more toxic to *Daphnia magna* than the parent FE (48 h EC_{50} of 4.2−6.9 mg/L). Thus, more toxic and photoresistant products were generated from photolysis of the herbicide. Ecotoxicological effects of phototransformed products from pesticides should be emphasized for the ecological risk assessment of these anthropogenic pollutants.

KEYWORDS: Fenoxaprop-*p*-ethyl; photolysis products; acute toxicity; *Daphnia magna*

INTRODUCTION

Among the chemical factors affecting the behavior of pesticides, photolysis is expected to be a major degradation process involved in dissipation in water, soils, and plants. More importantly, previous studies showed that some products generated from photolysis (*1, 2*) of pesticides were more toxic than the parent compounds. A significant example is the P = S to P = O conversion in organophosphorus insecticides. This sunlight-promoted conversion has been implicated as a cause of injury to farm workers (*3*). Therefore, assessing the ecological risk of a pesticide requires an understanding of its degradation pathway and toxicity of the products.

Fenoxaprop-*p*-ethyl (FE, ethyl 2-{4-[(6-chloro-2-benzoxazolyl)oxy]phenoxy}propanoate) is widely used in many counties and belongs to a large class of pesticides known as the aryloxyphenoxypropionate herbicides (*4*). As an acetyl-CoA carboxylase (ACCase) inhibitor, FE is intended for control of various annual perennial grass weeds in rice, wheat, soybeans, and turf (*5*). The metabolism of fenoxaprop-ethyl, the racemic mixture of the herbicide, in various plants has been studied, and its main degradation pathway was found to be hydrolysis forming fenoxaprop. At pH values between 4 and 10, hydrolysis of FE generated fenoxaprop-*p* (FA), ethyl 2-(4-hydroxyphenoxy) propanoate (EHPP) and 6-chloro-2,3-dihydrobenzoxazol-2-one (CDHB) (*6*). CDHB, EHPP, and fenoxaprop were also identified as photodegradation products of fenoxaprop-ethyl under fluorescent UV irradiation ($\lambda > 290$ nm) (*7*) and were less toxic to aquatic water flea *Daphnia magna* than the parent herbicide (*6*). CDHB can also be formed by biodegradation of fenoxaprop-ethyl, which was found to cause adverse effects on the growth of bacteria and fungi (*8, 9*).

In this study, we further investigated the photodegradation pathway of FE and emphasized the effects of irradiation wavelengths on the distribution of the photoproducts. The photolysis of 4-[(6-chloro-2-benzoxazolyl)oxy]phenol (CBOP), one of the main photodegradation products of FE, was also investigated. More importantly, *D. magna* was chosen to evaluate the acute toxicity of FE as well as its main transformation products. The results of the study can increase the understanding of the potential risks derived from the transformation products of pesticides and the emerging pollutants like pharmaceuticals and personal care products.

MATERIALS AND METHODS

Chemicals. FE (97%) was supplied by Ulrodragon Co. (Hangzhou, China). FA (97%) was purchased from Sigma-Aldrich. EHPP (98%) was purchased from Yongnuo Pharma. Ltd. (Nanjing, China). CDHB (97%) and CBOP (97%) were purchased from Tianchen Chemical Factory (Huai'an, China) and Lihua Research Institute Ltd. (Jiangshu, China), respectively. Photographic-grade hydroquinone (HQ, > 99%)

* To whom correspondence should be addressed. Tel/Fax: +86-411-8470 6269. E-mail: jwchen@dl.cn.

10.1021/jf801341s CCC: $40.75
Published on Web 08/07/2008

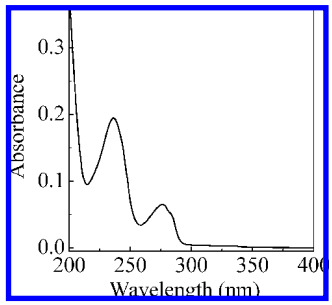

Figure 1. UV−vis spectra of FE in water and acetonitrile (10% v/v).

was a gift of Lianyungang Sanjili Chemical Industry Co. Ltd. (Lianyungang, China). The derivative reagent [*N*,*O*-Bis(trimethylsilyl) trifluoro acetamide (BSTFA) + trimethylchlorosilane (TMCS), 99:1, purity >99%] was purchased from Supelco (United States). Acetone, acetonitrile, and dichloromethane were high-performance liquid chromatography (HPLC) grade and purchased from Tedia Company (Fairfield, OH).

Photolysis Experiment. The irradiation experiments were performed using a 125 W high-pressure mercury lamp as a light source. The lamp was immersed inside a quartz glass well through which cold tap water flowed to keep the lamp cool. At the distance of 5 cm from the light source, a 500 mL quartz or Pyrex reactor was placed parallelly to get the irradiation of λ > 200 nm or λ > 290 nm, respectively. The light intensity was 1300 μW/cm^2 at 365 nm. To overcome solubility limitations, acetonitrile (5%) was added as a cosolvent to achieve an 1 mg/L initial concentration of FE. The same FE solution kept in the dark was used as a control.

Sunlight irradiation experiments were carried out on sunshiny days at Dalian (38° 53′ N, 12° 31′ E) in May 2005. The initial concentration of FE was 2 mg/L, and the cosolvent acetonitrile concentration was 10%. The solutions were filled into cylindrical quartz glass tubes (2 cm internal diameter) that were closed by septa, attached on a rack inclined about 30° from horizon, and exposed to solar light. Dark control experiments were performed the same way, but the tubes were wrapped in foil. UV−vis spectra of FE were recorded between 200 and 400 nm employing a Hitachi U2800 UV−vis spectrometer (**Figure 1**).

HPLC Analysis and Products Identification. Aliquots (1 mL) of the reaction solution were periodically sampled at designed intervals and analyzed immediately by an Agilent 1100 HPLC with a Hypersil C_{18} analytical column (5.0 μm, 4.6 mm × 250 mm). The flow rate of the mobile phase (acetonitrile:water, 70:30) was 1.0 mL/min, the injection volume was 10 μL, and the UV detection wavelength was 240 nm.

An Agilent 1100 HPLC/G2445A Ion-Trap MS and Agilent GC 6890N/5975 MSD were used to identify photolytic products. For the analysis, dichloromethane (20 mL) was used to extract the samples three times. The organic phases were combined, dried with anhydrous sodium sulfate, concentrated to about 1 mL by rotary evaporation, and then gently dried by nitrogen stream and reconstituted in 1 mL of acetonitrile. Electrospray ionization in positive and negative mode was performed for HPLC-MS/MS analysis. The mass scan range was *m*/*z* 100−600. For elution of photoproducts, the linear gradient profile of water/acetonitrile was adopted as follows: 0 min, 90% water and 10% acetonitrile; 30 min, 10% water and 90% acetonitrile.

For gas chromatography−mass spectrometry (GC-MS) analysis, derivatization of photodegradation products with BSTFA + TMCS was performed for 1 h at 70 °C; then, the derivatized solution was gently dried by nitrogen stream and reconstituted in 1 mL of *n*-hexane. The GC column was a HP-5 (30 m × 0.32 mm × 0.25 μm), and the temperature program was from 65 to 150 °C at a rate of 20 °C/min, then to 280 at 10 °C /min (*6*). The inlet temperature was 250 °C, and the injection volume was 1 μL with helium as a carrier gas. The mass spectrometer detector was operated at an ionization voltage of 70 eV and a source temperature of 200 °C in full scan mode from *m*/*z* 50 to 550.

Toxicity Assays. *D. magna* and *Chlorella pyrenoidosa* were cultivated for more than 5 years. *D. magna* were cultured in nonchlorinated and aerated tap water and fed with *C. pyrenoidosa* with a density of ca. 10^5 cells/mL. The photoperiod was 14:10 h (light:dark), and the temperature was 20 ± 1 °C (*6*).

The 48 h acute toxicity test of *D. magna* was carried out according to the standard testing procedure (*10*). On the basis of the range finding tests, five concentration treatments and a control without chemicals were adopted. The tests were performed in beakers each containing 100 mL of test solution and 10 neonates that were at least the third generation with ages less than 24 h. All of the assays were repeated in triplicate. The tested compounds were poorly water-soluble except HQ, so dimethyl sulfoxide (DMSO) was used as a solubilizing agent with the final concentration not exceeding 0.1% (v/v). Solvent controls (dilution water with 1 mL/L DMSO) exhibited no acute toxicity on *D. magna*. Immobilization of *D. magna* was recorded at 48 h if no movement occurred after gentle stirring of the test solutions within 15 s. The median effective concentration (EC_{50}) was calculated as a typical end point, and Probit analysis (U.S. EPA, 1993) was adopted to estimate the 48 h EC_{50} and its 95% confidence limits (CL). For the control of the toxicity assay, the 24 h EC_{50} of the reference compound $K_2Cr_2O_7$ was determined periodically, which varied between 0.7 and 1.1 mg/L.

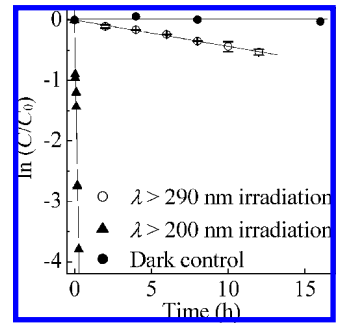

Figure 2. Kinetics of photolysis of FE under irradiation at λ > 200 nm (quartz reactor) and λ > 290 nm (Pyrex reactor).

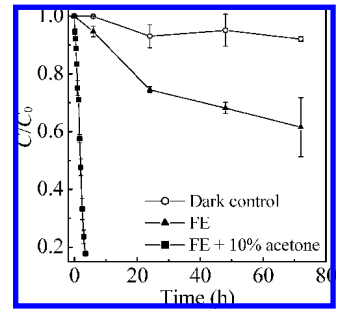

Figure 3. Kinetics of photolysis of FE under irradiation of sunlight.

RESULTS AND DISCUSSION

Photolysis Kinetics. The experimental results indicated that the first-order kinetics could be used to describe the photolysis of FE in water. All of the dark control tests showed negligible loss of FE. As expected, FE photodegraded much faster in the quartz reactor than in the Pyrex reactor, and the photolysis rate constants were 310 times faster at λ > 200 nm irradiation than at λ > 290 nm (**Figure 2**), confirming that the spectrum match between the light source and the absorption spectrum (**Figure 1**) was a decisive factor of the photolysis rates.

Under the irradiation of sunlight on sunny days (May 2005), FE photodegraded slowly, and 72 h irradiation resulted in 38% loss of FE (**Figure 3**), which is due to the low intensity of sunlight at λ < 320 nm. The addition of 10% (v/v) acetone increased the photolysis rate greatly, and 3.5 h irradiation resulted in 88% loss of FE. Acetone absorbs sunlight and can act as a sensitizer for the photolysis of many aqueous organic pollutants (*11, 12*). The observation implies that the excited state

Table 1. GC-MS Spectrum of FE and Its Photoproducts

products	retention time (min)	mass spectral data (*m/z*) (% relative abundance)	MW (TMS)
BOA	9.35	135 (100), 79 (38), 52 (20), 91 (15), 64 (11)	135
CDHB	11.74	169 (100), 171 (33), 125 (12), 113 (30), 78 (33), 63 (9.8)	169
EHPP	10.76	210 (69), 137 (90), 110 (100), 93 (9), 81 (27), 65 (18)	210
CBOP	17.17	261 (100), 263 (33), 170 (16), 93 (14), 82 (33), 65 (35)	261
FE isomer	21.61	361 (16), 288 (6), 260 (100), 232 (5), 204 (4), 63 (4)	361
HQ	7.24	182 (48), 167(100), 73 (10), 61 (4)	110 (182)
HDHB	13.31	223 (74), 208 (100), 164 (5), 137 (8), 73 (30)	151 (223)
HBOP	18.96	387 (100), 372 (17), 193 (15), 178 (12), 135 (9), 73 (73)	243 (387)
EBP	19.31	399 (61), 384 (22), 356 (22), 326 (100), 97 (14), 73 (87)	327 (399)
lactone	19.56	315 (81), 317 (28), 287 (100), 91 (35), 65 (33)	315
EHBP	22.50	415 (100), 342 (30), 125 (5), 97 (18), 73 (53)	343 (415)
EHBP isomer	24.07	415 (14), 342 (4), 314 (100), 315 (24), 73 (13)	343 (415)
FE	20.30	361 (71), 288 (100), 261 (26), 76 (15), 119 (14), 75 (24)	361

of acetone could transfer the excited energy to FE and lead to an excited state of FE that subsequently photolyzes (*12, 13*). In natural water bodies, dissolved organic matter (*14*), algaes (*Chlorella vulgaris*, *Chlamydomonas sajao*, or *Anabaena cylindrica*) (*15, 16*), and some inorganic ions (nitrate, bicarbonate, or ferric iron) (*14, 17*) may also act as sensitizers to promote the photolysis of FE, which needs further investigation.

Photolysis Products. The photoproducts were the same under the irradiation at $\lambda > 200$ nm and $\lambda > 290$ nm, which can be confirmed by GC-MS. The mass spectral information of FE and its photoproducts is listed in **Table 1**.

The derivatization technique was successful in determining the photoproducts of FE. The products containing a trimethylsilyl structure exhibited typical ion fragments of $M - CH_3$ and $m/z = 73$. The latter has been identified as $C_3H_9Si^+$. Both derivatization and nonderivatization of benzoxazolin-2(3*H*)-one (BOA), ethyl 2-{4-[(2-benzoxazolyl)oxy]phenoxy}propanoate (EBP), CDHB, EHPP, CBOP, and FE isomer were detected. BOA and HQ were positively confirmed by the NIST05a library with high spectrographic fit (>93%). CDHB, EHPP, CBOP, FA, and FE were in good accordance with the HPLC retention time of the pure chemicals. HPLC-MS/MS analysis confirmed the formation of BOA, CBOP, 6-hydroxy-2,3-dihydrobenzoxazol-2-one (HDHB), 4-[(6-hydroxy-2-benzoxazolyl)oxy]phenol (HBOP), and ethyl 2-[4-[(6-hydroxy-2-benzoxazolyl) oxy]phenoxy]propanoate (EHBP) or EHBP isomer. The lactone is tentatively identified by interpretation of the mass spectrum (see the Supporting Information).

CBOP, derived from cleavage of the phenoxy-propanoate ether linkage of FE, was the main photoproduct under both $\lambda > 200$ nm and $\lambda > 290$ nm irradiation conditions. However, as shown in **Figure 4**, CBOP was almost resistant to photolysis at irradiation of $\lambda > 290$ nm, and the photolysis rate was seven times slower than the parent FE under the irradiation of $\lambda > 200$ nm. Thus, CBOP is a more photochemically stable product than FE, which is likely to accumulate in natural waters.

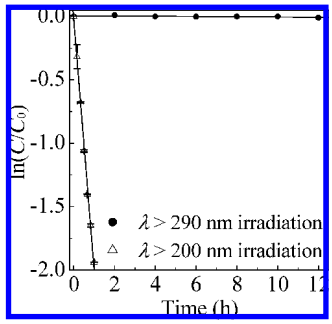

Figure 4. Kinetics of photolysis of CBOP under irradiation at $\lambda > 200$ nm (quartz reactor) and $\lambda > 290$ nm (Pyrex reactor).

CDHB and EHPP were derived from the breakdown of another ether linkage, the benzoxazolyl-oxy-phenyl bond of FE. Studies on the hydrolysis of FE (*6*) and transformation in soil of fenoxaprop-ethyl (*18*) also revealed that the herbicide can yield these two products. EHBP was a 6-OH analogue of FE, resulting from the conversion of −Cl to −OH on the phenyl ring. The photoconversion was accompanied with the formation of HCl, which was proved by the decrease of pH from 6.3 to 5.5 for the FE solution at $\lambda > 200$ nm irradiation (82% of FE was degraded) and from 6.3 to 5.0 at $\lambda > 290$ nm irradiation (96% of FE was degraded). The hydroxylation is a typical reaction in aqueous solutions for photodegradation of phenoxypropionate herbicides, such as 2,4-D and MCPA (*19, 20*).

FA was generated through the ethyl−ester bond cleavage of FE, which was a primary degradation process for FE (*21, 22*). The desterified metabolite FA is phytotoxic and about 100 times more powerful than fenoxaprop-ethyl in inhibiting ACCase (*23*). FE isomer resulted from the radical rearrangement reaction of FE (*20*). This reaction was previously reported for mecoprop (*24*) and dichlorprop (*25*). FE isomer can undergo photohydrolysis, photoreduction, and elimination of alcohol to generate EHBP isomer, EBP, and lactone, respectively. **Figure 5** shows that the main photoproducts were finally photodegraded under the irradiation of $\lambda > 200$ nm in parallel with the parent herbicide.

On the basis of the identified photoproducts, the photodegradation pathways of FE are outlined via the following processes: rearrangement, loss of ethanol after rearrangement, de-esterification, dechlorination, hydroxylation, and the cleavage of the ether linkages (**Figure 6**). BOA, HQ, HDHB, and HBOP were formed by further photodegradation of the metabolites of FE through the same processes as the parent herbicide. Noticeably, with the irradiation of $\lambda > 290$ nm, HBOP can not be generated from CBOP that was stable under the irradiation condition. Toole (*7*) suggested that photolysis of fenoxaprop-

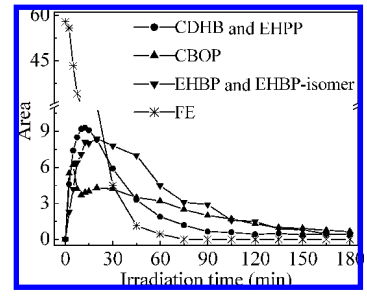

Figure 5. Evolution of FE and its main photoproducts during direct photolysis under irradiation at $\lambda > 200$ nm. The peak areas were determined at 240 nm of diode array detector.

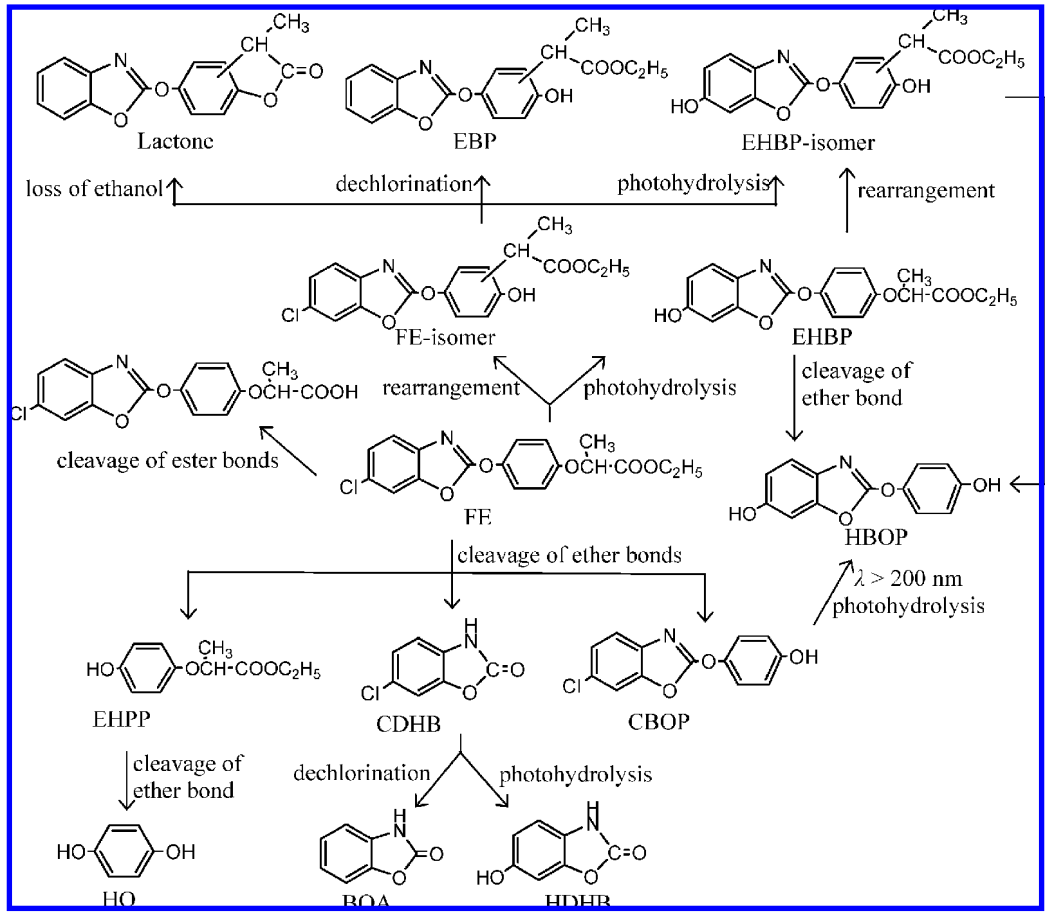

Figure 6. Proposed photolysis pathway of FE.

Table 2. Acute Immobilization Data to *D. magna* for the Tested Compounds

compounds	48 h EC_{50} (95% CL) (mg/L)
FE[a]	5.29 (4.62−6.63)
HQ	0.266 (0.248−0.284)
CBOP	1.56 (1.49−1.64)
FA[a]	14.6 (13.0−16.5)
CDHB[a]	8.4 (8.0−8.7)
EHPP[a]	70.0 (58.4−83.3)
BOA[b]	>2

[a] Data from Lin et al. (*6*). [b] Data from Fritz et al. (*8*).

ethyl also led to a small amount of 2-(4-hydroxyphenoxy) propionate (HPP) that was not affirmed by this study. This may account for the low production and high polarity of HPP.

Toxicity of FE and Its Photoproducts to *D. magna*. **Table 2** summarizes the 48 h EC_{50} values and the corresponding 95% CLs of FE and the tested photoproducts. According to the EC_{50} values, HQ and CBOP are more toxic than the parent compound. The control experiments performed in *D. magna*-free solutions showed negligible loss of the test chemicals except for HQ, which changed solution color in 24 h. HQ was susceptible to oxidation to 1,4-benzoquinone (*26*) that is considered to be an arylating electrophile (*27*); thus, the determined EC_{50} of HQ may not accurately describe the toxicity. CBOP is more toxic than FE with a factor of ca. 3. Increased toxicity of phenolic metabolites of other aryloxypropionic acid herbicides has also been reported (*28, 29*).

The EC_{50} value of BOA was higher than its solubility limit, as was found by Fritz et al. (*8*). However, BOA is known as a wheat allelochemical and slightly inhibits the growth of onion, tomato, and cress roots at the concentration of 10^{-3} M (*30*). The modes of action for BOA are complicated, including an integrity disruption at a radicular cell membrane system, changes in ATPase activity, and oxidative stress (*31*). Therefore, it is hard to exclude the adverse effect of BOA to organisms, although it has a low acute toxicity. FA, CDHB, and EHPP are less toxic than the parent compound. However, CDHB may have a different but more potent mode of toxic action than FE (*6*).

ACKNOWLEDGMENT

The study was supported by the National Basic Research Program of China (Project 2006CB403302) and the National Natural Science Foundation (no. 20337020) of China.

Supporting Information Available: GC-MS and HPLC-MS/MS spectra of FE and its photoproducts. This material is available free of charge via the Internet at http://pubs.acs.org.

LITERATURE CITED

(1) Blaha, L.; Klanova, J.; Klan, P.; Janosek, J.; Skarek, M.; Ruzicka, R. Toxicity increases in ice containing monochlorophenols upon photolysis: Environmental consequences. *Environ. Sci. Technol.* **2004**, *38* (10), 2873–2878.

(2) Bonnemoy, F.; Lavedrine, B.; Boulkamh, A. Influence of UV irradiation on the toxicity of phenylurea herbicides using Microtox test. *Chemosphere* **2004**, *54* (8), 1183–1187.

(3) Miller, G. C.; Crosby, D. G. Pesticide photoproducts: Generation and significance. *J. Toxicol. Clin. Toxicol.* **1982**, *19* (6−7), 707–735.

(4) Cocker, K. M.; Moss, S. R.; Coleman, J. O. D. Multiple mechanisms of resistance to fenoxaprop-*p*-ethyl in United Kingdom and other European populations of herbicide-resistant *Alope-*

curus myosuroides (Black-Grass). *Pestic. Biochem. Physiol.* **1999**, *65* (3), 169–180.
(5) Tal, A.; Romano, M. L.; Stephenson, G. R.; Schwan, A. L.; Hall, J. C. Glutathione conjugation: A detoxification pathway for fenoxaprop-ethyl in barley, crabgrassl, oat, and wheat. *Pestic. Biochem. Physiol.* **1993**, *46* (3), 190–199.
(6) Lin, J.; Chen, J. W.; Cai, X. Y.; Qiao, X. L.; Huang, L. P.; Wang, D.; Wang, Z. Evolution of toxicity upon hydrolysis of fenoxaprop-*p*-ethyl. *J. Agric. Food Chem.* **2007**, *55* (18), 7626–7629.
(7) Toole, A. P.; Crosby, D. G. Environmental persistence and fate of feoxaprop-ethyl. *Environ. Toxicol. Chem.* **1989**, *8*, 1171–1176.
(8) Bravo, H. R.; Copaja, S. V.; Lazo, W. Antimicrobial activity of natural 2-benzoxazolinones and related derivatives. *J. Agric. Food Chem.* **1997**, *45* (8), 3255–3257.
(9) Hoagland, R. E.; Zablotowicz, R. M. Biotransformations of fenoxaprop-ethyl by fluorescent *Pseudomonas* strains. *J. Agric. Food. Chem.* **1998**, *46* (11), 4759–4765.
(10) OECD. *Guidelines for Testing Chemicals. 202. Daphnia sp. Acute Immobilization Test and Reproduction Test*; Organisation for Economic Co-operation and Development: París, 1984.
(11) Liu, S. Z.; Li, Q. X. Photolysis of spinosyns in seawater, stream water and various aqueous solutions. *Chemosphere* **2004**, *56* (11), 1121–1127.
(12) Tissot, A.; Boule, P.; Lemaire, J. Photochemistry and environment. VII. The photohydrolysis of chlorobenzene. Studies of the excited state involved. *Chemosphere* **1984**, *13* (3), 381–389.
(13) Chu, W.; Tsui, S. M. Photoreductive model of disperse orange 11 in aqueous acetone and triethylamine. *J. Environ. Eng. ASCE* **2001**, *127* (8), 741–747.
(14) Walse, S. S.; Morgan, S. L.; Kong, L.; Ferry, J. L. Role of dissolved organic matter, nitrate, and bicarbonate in the photolysis of aqueous fipronil. *Environ. Sci. Technol.* **2004**, *38* (14), 3908–3915.
(15) Peng, Z.; Wu, F.; Deng, N. S. Photodegradation of bisphenol A in simulated lake water containing algae, humic acid and ferric ions. *Environ. Pollut.* **2006**, *144* (3), 840–846.
(16) Wang, L.; Zhang, C. B.; Wu, F.; Deng, N. S. Photodegradation of aniline in aqueous suspensions of microalgae. *J. Photochem. Photobiol. B* **2007**, *87* (1), 49–57.
(17) Fisher, J. M.; Reese, J. G.; Pellechia, P. J.; Moeller, P. L.; Ferry, J. L. Role of Fe(III), phosphate, dissolved organic matter, and nitrate during the photodegradation of domoic acid in the marine environment. *Environ. Sci. Technol.* **2006**, *40* (7), 2200–2205.
(18) Smith, A. E. Persistence and transformation of the herbicides [^{14}C]fenoxaprop-ethyl and [^{14}C]fenthiaprop-ethyl in two prairie soils under laboratory and field conditions. *J. Agric. Food Chem.* **1985**, *33* (3), 483–488.
(19) Zepp, R. G.; Lee Wolfe, N.; Gordon, J. A.; Baughman, G. L. Dynamics of 2, 4-D esters in surface waters: hydrolysis, photolysis, and vaporization. *Environ. Sci. Technol.* **1975**, *9* (13), 1144–1150.
(20) Zertal, A.; Sehili, T.; Boulle, P. Photochemical behaviour of 4-chloro-2-methylphenoxyacetic acids—Influence of pH and irradiation wavelength. *J. Photochem. Photobiol. A* **2001**, *146* (1–2), 37–48.
(21) Zablotowicz, R. M.; Hoagland, R. E.; Staddon, W. J.; Locke, M. A. Effects of pH on chemical stability and de-esterification of fenoxaprop-ethyl by purified enzymes, bacterial extracts, and soils. *J. Agric. Food Chem.* **2000**, *48* (10), 4711–4716.
(22) Hoagland, R. E.; Zablotowicz, R. M. Biotransformations of fenoxaprop-ethyl by fluorescent *Pseudomonas* strains. *J. Agric. Food Chem.* **1998**, *46* (11), 4759–4765.
(23) Yaacoby, T.; Hall, J. C.; Stephenson, G. R. Influence of fenchlorazole-ethyl on the metabolism of fenoxaprop-ethyl in wheat, barley, and crabgrass. *Pestic. Biochem. Physiol.* **1991**, *41*, 296–304.
(24) Meunier, L.; Boule, P. Direct and induced phototransformation of mecoprop [2-(4-chloro-2-methylphenoxy)propionic acid] in aqueous solution. *Pest Manage. Sci.* **2000**, *56* (12), 1077–1085.
(25) Climent, M. J.; Miranda, M. A. Photodegradation of dichlorprop and 2-naphthoxyacetic acid in water. Combined GC-MS and GC-FTIR study. *J. Agric. Food Chem.* **1997**, *45* (5), 1916–1919.
(26) Schuurmann, G.; Aptula, A. O.; Kuhne, R.; Ebert, R. U. Stepwise discrimination between four modes of toxic action of phenols in the *Tetrahymena pyriformis* assay. *Chem. Res. Toxicol.* **2003**, *16* (8), 974–987.
(27) Schultz, T. W.; Sinks, G. D.; Cronin, M. T. D. Quinone-induced toxicity to *Tetrahymena*: Structure−activity relationships. *Aquat. Toxicol.* **1997**, *39* (3−4), 267–278.
(28) Cai, X. Y.; Liu, W. P.; Jin, M. Q.; Lin, K. D. Relation of diclofop-methyl toxicity and degradation in algae cultures. *Environ. Toxicol. Chem.* **2007**, *26* (5), 970–975.
(29) DeLorenzo, M. E.; Scott, G. I.; Ross, P. E. Toxicity of pesticides to aquatic microorganisms: A review. *Environ. Toxicol. Chem.* **2001**, *20* (1), 84–98.
(30) Macias, F. A.; Marin, D.; Oliveros-Bastidas, A.; Castellano, D.; Simonet, A. M.; Molinillo, J. M. G. Structure−activity relationships (SAR) studies of benzoxazinones, their degradation products and analogues. Phytotoxicity on standard target species (STS). *J. Agric. Food Chem.* **2005**, *53* (3), 538–548.
(31) Jia, C. H.; Kudsk, P.; Mathiassen, S. K. Joint action of benzoxazinone derivatives and phenolic acids. *J. Agric. Food Chem.* **2006**, *54* (11), 1049–1057.

Received for review April 30, 2008. Revised manuscript received July 7, 2008. Accepted July 8, 2008.

JF801341S